Rare Metal Materials and Engineering
Volume 52, Issue 1, January 2023
Available online at www.rmme.ac.cn

Science Press

Cite this article as: Li Yongquan, Tian Xingda, Wang Cunxi, et al. Influence of Y_2O_3 on Microstructures and Oxidation Resistance of Cr-Al-Y Coatings Prepared via Pack Cementation on DZ125 Alloy[J]. Rare Metal Materials and Engineering, 2023, 52(01): 48-53.

ARTICLE

Influence of Y_2O_3 on Microstructures and Oxidation Resistance of Cr-Al-Y Coatings Prepared via Pack Cementation on DZ125 Alloy

Li Yongquan[1,2], Tian Xingda[2], Wang Cunxi[2], Li Xuan[3], Yang Shaolin[2]

[1] School of Mechatronic Engineering, North Minzu University, Yinchuan 750021, China; [2] School of Materials Science & Engineering, North Minzu University, Yinchuan 750021, China; [3] College of Mechanical Engineering, Sichuan University of Science and Engineering, Zigong 643000, China

Abstract: To further improve the high-temperature service performance of DZ125 alloy, the rare earth element Y-modified Cr-Al co-deposition coating was prepared via the pack cementation method on the DZ125 alloy surface. The effects of Y_2O_3 content on the oxidation resistance at high temperature and the microstructure and phases of the co-deposition coating were studied. Results show that the Cr-Al-Y coatings prepared under different conditions have a triple-layered structure, which is arranged from the outside to the inside as follows: the Cr+Ni_3Cr_2 outer layer, the Ni_3Cr_2+$Al_{13}Co_4$ middle layer, and the Ni_3Al inner layer. Both the coating thickness and the density are strongly increased with the addition of 0wt%−2wt% Y_2O_3, and they are decreased when the content of Y_2O_3 is further increased to 5wt%. The results of oxidation tests at 1100 °C demonstrate that the Cr-Al-Y coating significantly improves the oxidation resistance of DZ125 alloy at high temperatures.

Key words: DZ125 alloy; Y-modified Cr-Al coating; Y_2O_3; oxidation resistance at high temperature

As a directional-solidified nickel-based superalloy, DZ125 alloy is widely applied for aero-engine blades and gas turbine[1]. However, the service life and safety stability of the equipment of DZ125 alloy are strongly influenced by the high-temperature environment and gas corrosion[2–3]. Although alloying can effectively enhance its high-temperature oxidation resistance, the comprehensive properties of DZ125 alloy, including the high-temperature strength and melting point, will be reduced after the addition of alloying elements[4]. Since these failures usually occur on the material surface, a protective coating is required on DZ125 alloy for high-temperature applications[5].

In the past decades, various surface modification techniques have been developed to prepare protective coatings on DZ125 alloys, such as electron beam physical vapor deposition (EB-PVD)[6–7], plasma spraying[8], and pack cementation[9]. Among them, the pack cementation method, including the chromizing, siliconization, aluminizing, and co-diffusion coatings, is effective and easy to operate. Particularly, the formation of protective Al_2O_3 scale can improve the surface properties of nickel, niobium, and titanium components[10–11]. However, the long-term service of aluminide coatings at high temperatures is hindered by the cracks and brittleness of coatings. Therefore, the addition of Cr, Si, Zr, Co, Hf, and Y elements has been used to ameliorate the stability of protective oxide scale on DZ125 alloy[12–15]. Among these elements, Y and Cr are beneficial to reduce the grain size and increase the thickness and oxidation resistance of the coatings[16]. Li et al[17–18] found that the Y_2O_3 addition can promote the Al diffusion and improve the oxidation resistance of the coating. Lin et al[19–20] revealed that the Y_2O_3 addition can accelerate the Cr diffusion and enhance the corrosion resistance of the coating. Qiao et al[21] improved the oxidation resistance of NbTiSi-based alloy through applying the Cr-Si coatings.

Received date: April 18, 2022
Foundation item: Natural Science Foundation of Ningxia (2022AAC03224); National Natural Science Foundation of China (51961003, 52161009); Major Project of Science and Technology Department of Sichuan Province (2022YFSY0036)
Corresponding author: Li Yongquan, Ph. D., Associate Professor, School of Mechatronic Engineering, North Minzu University, Yinchuan 750021, P. R. China, Tel: 0086-951-2067378, E-mail: 2014141@nmu.edu.cn

In this research, the Y-modified Cr-Al coatings were prepared on the nickel-based DZ125 superalloy by the halide-activated pack cementation (HAPC) method. The influences of rare earth (RE) element addition on the structure, phase constituents, formation mechanism, and oxidation behavior at 1100 °C of the coatings were characterized.

1 Experiment

The nominal composition of DZ125 alloy was Ni - 10.0Co -8.9Cr - 7.5W - 3.8Ta - 1.6Mo - 5.3Al - 1.5Hf - 0.8Ti - 0.09C - 0.015B(at%). The DZ125 alloy specimens of 15 mm×15 mm× 15 mm was cut by the electro-discharge machining, polished by 1500# SiC-grit papers, and then washed with acetone through the ultrasonication bath for 20 min.

According to Ref. [15, 17 – 18], the used pack mixture consisted of 4Al-10Cr-$m$$Y_2O_3-7NH_4$C-(79−$m$)$Y_2O_3$ (wt%, m= 0, 2, 5) alloy. Al, Cr, and Y_2O_3 were used as the donor sources, Y_2O_3 was used as the filler, and NH_4Cl as the activator. These powders were ground in a planetary ball mill for 4 h to ensure the mixing and refinement effects. The DZ125 alloy specimens were buried by the mixed powder in an alumina crucible which was sealed by the Y_2O_3-based silica sol binder. The crucible was heated in a furnace to 1050 °C at the heating rate of 15 °C·min^{-1}, kept at co-deposition temperature for 2 h, and finally air-cooled to room temperature.

According to the actual service environment of DZ125 alloy, the oxidation behavior of DZ125 alloy with coatings with/without Y_2O_3 was tested isothermally at 1100 °C under static air environment in an electric furnace. The specimen was placed in an alumina crucible, and the mass gains of the oxidized specimens were calculated by electronic balance. Moreover, to reduce experiment error, the oxidation tests were conducted three times.

The phases of the coating and oxidized specimens were characterized by X-ray diffractometer (XRD, Panalytical X'Pert PRO, Japan, Cu Kα radiation, scanning rate of 4°/min). The chemical composition and cross-section microstructure of the constituent phases were analyzed by field-emission scanning electron microscope (SEM, ZEISS SIGMA 500/VP) coupled with energy dispersive spectrometer (EDS).

2 Results and Discussion

2.1 Coating structure

Fig. 1 shows the thickness of different Cr-Al-Y co-deposition coatings prepared at 1050 °C for 2 h. The coating thickness is increased obviously from 18.0 μm to 31.2 μm with increasing the Y_2O_3 content from 0wt% to 2wt%, and then decreased to 23.5 μm with further increasing the Y_2O_3 content to 5wt%.

Fig. 2 presents the cross-section morphologies and element distributions of different Cr-Al-Y coatings. The three-layered coatings can be clearly observed in all the Cr-Al-Y coatings. As shown in Fig.2a, the Cr-Al-Y coating without Y_2O_3 has the outer layer, middle layer, and inner layer with thickness of 5.1, 7.7, and 5.2 μm, respectively. The outer layer has a few holes,

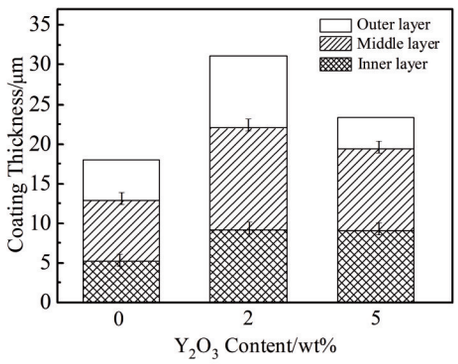

Fig.1 Thickness of different Cr-Al-Y co-deposition coatings prepared at 1050 °C for 2 h

and it is not uniform in thickness. The discontinuous inner layer is broken by the Kirkendall caverns. EDS analysis results of the Cr-Al-Y coating without Y_2O_3 reveal that the 59.4at% – 63.2at% Cr exists in the outer layer. According to XRD patterns in Fig.3, the outer layer of the Cr-Al-Y coating is composed of Cr and Ni_3Cr_2 phases. The middle layer consists of dark grey tissue with a large amount of Ni and Cr and a small amount of Al and Co, as shown in Fig. 2d. XRD pattern in Fig. 4 suggests that the main composition of the middle layer is Ni_3Cr_2 and $Al_{13}Co_4$.

As shown in Fig.2b, the Cr-Al-Y coating with 2wt% Y_2O_3 is composed of an outer layer, a thick middle layer, and a thick inner layer with the thickness of 9.1, 12.8, and 9.2 μm, respectively. The outer layer has uniform thickness and dense structure. EDS analysis results of the Cr-Al-Y coating with 2wt% Y_2O_3 (Fig.2e) confirm that the Cr and Ni contents in the outer layer are 85.6at% – 88.6at% and 6.8at% – 8.0at%, respectively, while Y content is 0.7at%–0.9at%. XRD pattern of the outer layer of Cr-Al-Y coating with 2wt% Y_2O_3 (Fig.3) confirms that the outer layer mainly consists of Cr and Ni_3Cr_2 phases. Beneath the outer layer, the interleaved morphology can be observed in the middle layer, which contains a large amount of Ni and Cr and a small amount of Al and Co (Fig. 2e). This result is similar to that of the Cr-Al-Y coating with 0wt% Y_2O_3, i. e., the middle layer of Cr-Al-Y coating with 2wt% Y_2O_3 is composed of Ni_3Cr_2 and $Al_{13}Co_4$.

It can be found from Fig. 2c that the Cr-Al-Y coating with 5wt% Y_2O_3 consists of an outer layer, a middle layer, and a thick inner layer with the thickness of 3.9, 10.3, and 9.1 μm, respectively. EDS analysis results in Fig. 2f demonstrate that the outer layer consists of 88.1Cr-9.7Ni-0.6Al-0.5Co-1.1Y (at%). According to Fig. 3, the outer layer is composed of Cr and Ni_3Cr_2 phases, the Y content in this layer is increased to 1.1at%, and the coating thickness and density are decreased. Notably, Y or its compounds cannot be detected by XRD, which may be because the rare earth element Y in the coating exists as the solid solution of low content.

EDS analysis results in Fig. 2 reveal that the inner layers of Cr-Al-Y coatings with different Y_2O_3 contents are similar to each other. Thus, the inner layer of the Cr-Al-Y coating with

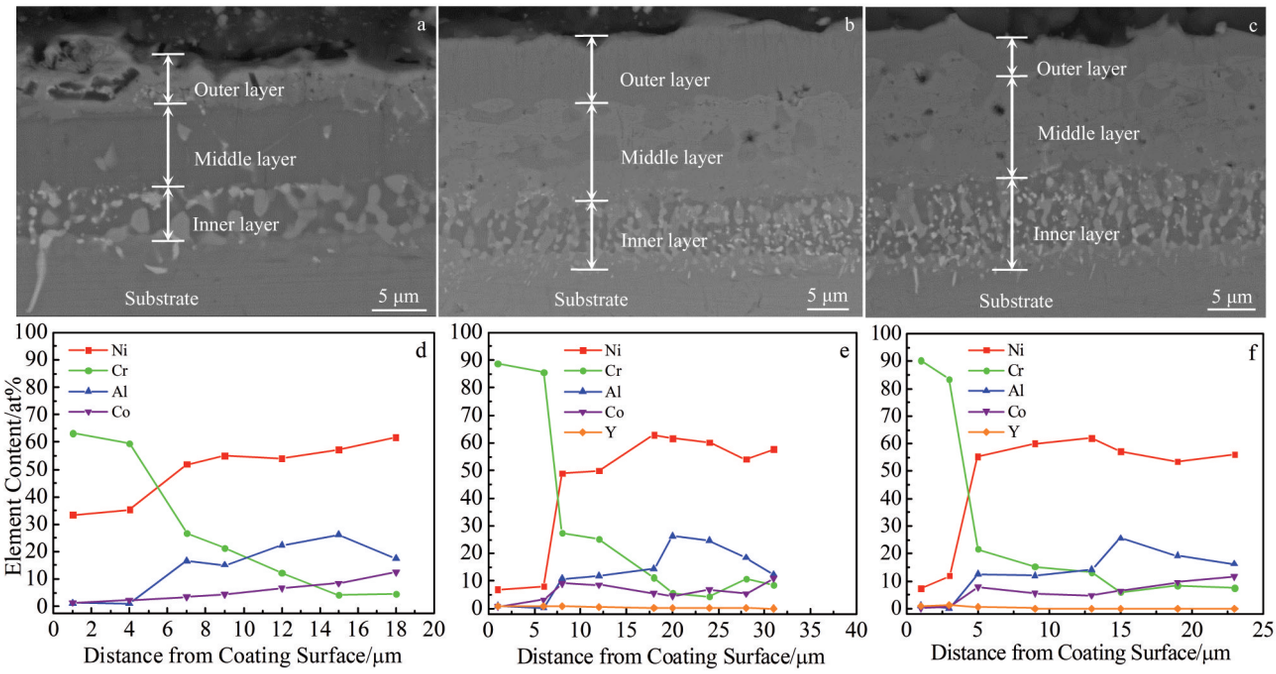

Fig.2 Cross-section morphologies (a–c) and element distributions (d–f) of Cr-Al-Y coatings with different Y_2O_3 contents: (a, d) 0wt%; (b, e) 2wt%; (c, f) 5wt%

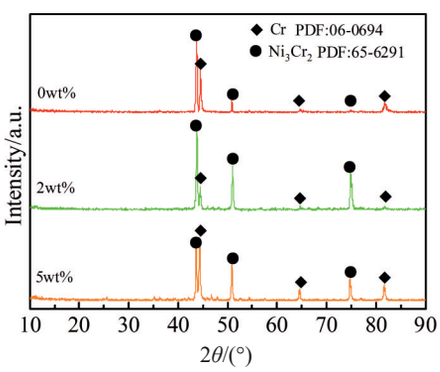

Fig.3 XRD patterns of different Cr-Al-Y coatings

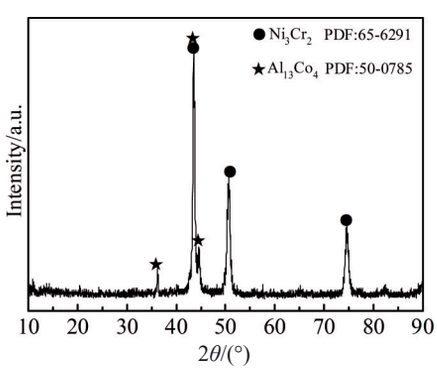

Fig.4 XRD pattern of the middle layer of Cr-Al-Y coating without Y_2O_3

2wt% Y_2O_3 is selected as a representative for further investigation. Fig.5a shows SEM morphology at backscattered electron (BSE) mode of the inner layer of Cr-Al-Y coating with 2wt% Y_2O_3, and it can be seen that the inner layer is composed of the light-gray (point 1) and gray (point 2) blocks with some dispersed white particles (point 3). Table 1 shows that the light-gray and gray blocks as well as the white particles have similar Ni and Al contents of about 58.8at% and 19.3at%, respectively. The Cr content in the light-gray blocks is about 15.7at%, and the white particles contain more Ta and W of about 2.7at% and 4.9at%, respectively. XRD pattern in Fig.5b indicates that the inner layer consists of Ni_3Al.

2.2 Structure formation of Cr-Al-Y coating

It can be deduced from Fig.2 that the coating is formed by depositing Al firstly and then depositing Cr. The effect of rare earth element in the pack cementation process can be explained as follows. When the rare earth element is added into the pack powder, Y atom infiltration results in lattice distortion due to the large atomic radius of Y element, thereby increasing the dislocation density and vacancy and accelerating the diffusion rate of Al and Cr atoms. Thus, the thickness of Cr-Al-Y coating with Y_2O_3 is thicker than that without Y_2O_3. However, excessive Y_2O_3 addition may lead to the adsorption of a large number of Y atoms on the substrate surface[22], therefore hindering the absorption of Cr and Al atoms on the substrate surface and resulting in the thinner coating, as shown in Fig.2c.

2.3 Oxidation behavior of Cr-Al-Y coating

2.3.1 Oxidation kinetics

The Cr-Al-Y coatings with 0wt% and 2wt% Y_2O_3 were selected for oxidation tests at 1100 °C in air. The mass changes of coated specimens and bare DZ125 alloy after the oxidation tests are shown in Fig. 6. The mass gain of the

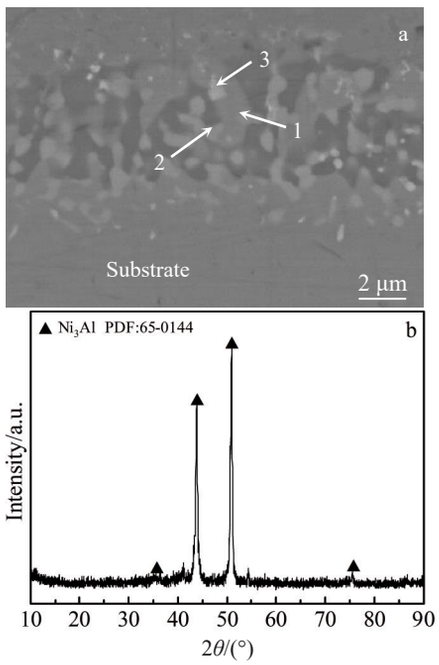

Fig.5 SEM-BSE cross-section morphology (a) and XRD pattern (b) of the inner layer in Cr-Al-Y coating with 2wt% Y_2O_3

coated specimens is nearly linear to the square root of oxidation time, regardless of the Y_2O_3 addition, which suggests that the oxidation behavior of coating obeys a parabolic law. It should be mentioned that there is no significant difference in the mass gain of the coated specimen with and without Y_2O_3 addition at the initial oxidation stage. However, the mass gain of the coated specimen without Y_2O_3 addition is obviously more than that with Y_2O_3 addition with prolonging the oxidation time to 10 h. The parabolic rate constant of the mass gain curves of DZ125 alloys with coating of 0wt% and 2wt% Y_2O_3 is about 4.76×10^{-3} and 2.02×10^{-3} $mg^2\cdot cm^{-4}\cdot h^{-1}$, respectively. In com-parison, the mass gain curve of DZ125 alloy has two distinctive parts: the parabolic rate constant is about 1.37×10^{-2} $mg^2\cdot cm^{-4}\cdot h^{-1}$ within 30 h and 4.71×10^{2} $mg^2\cdot cm^{-4}\cdot h^{-1}$ beyond 30 h of oxidation. This result infers that the fast oxidation occurs after proceeding for 30 h. Therefore, the high-temperature oxidation resistance of the DZ125 alloy is significantly improved by the coating with 2wt% Y_2O_3 addition. The oxidation resistance of DZ125 alloy with coating without Y_2O_3 addition is better than that of the bare DZ125 alloy, but it is worse than that with 2wt% Y_2O_3 addition.

2.3.2 Morphology of oxide scale

Fig. 7 presents SEM-BSE cross-section morphologies and XRD patterns of DZ125 alloys with/without coatings after oxidation at 1100 °C. According to Fig. 7a, the oxide scale formed on the bare DZ125 alloy surface is about 33 μm in thickness, and the cracks appear between the outer layer and the middle layer. EDS analysis results of point 1 in Fig. 7a demonstrate that the O and Cr contents in the outer layer of the oxide scale are 58.5at% and 32.3at%, respectively. XRD pattern in Fig.7d demonstrates that the outer layer of the oxide scale is mainly composed of Cr_2O_3, and the appearance of NiO and $NiCr_2O_4$ results from the fact that the oxide scale is destroyed after oxidation for 30 h. Therefore, partial Cr_2O_3 peels off from the outer layer and the middle layer of the oxide scale is exposed in environment. The contents of O and Ni in the middle layer of oxide scale (point 2) are about 55.1at% and 39.4at% , respectively, which indicates the existence of NiO and $NiCr_2O_4$. EDS analysis results of the inner layer of oxide scale (point 3) show that the ratio of Al:O ≈2:3, suggesting the Al_2O_3 layer.

As shown in Fig. 7b, the oxide scale on the surface of DZ125 alloy with 2wt% Y_2O_3 coating is very dense and fully adherent to the coating, and it is about 12 μm in thickness. EDS analysis result determines that the composition of the oxide scale (point 4) is 64.8O-16.1Al-18.5Cr-0.6Ti (at%). XRD pattern in Fig. 7e further proves that the oxide scale is probably composed of Cr_2O_3 and Al_2O_3. The formation of Al_2O_3 in the oxide scale during oxidation at 1100 °C originates from the outward Al diffusion from the Al-rich middle and inner layers to the coating surface. It is worth noting that some light-gray particles (point 5) can be observed between the oxide scale and the coating, and the Y content in those particles is as high as 1.2at%.

Fig. 7c shows the cross-section morphology of the DZ125 alloy with coating without Y addition after oxidation at 1100 °C for 100 h. The oxide scale formed on the coating surface is about 13 μm in thickness, and numerous pores and cracks form between the oxide scale and the coating. EDS analysis results reveal that the composition of oxide scale is 63.0O-18.8Al-17.6Cr-0.6Ti (at%). XRD pattern in Fig. 7f further confirms that the oxide scale is mainly composed of Cr_2O_3 and Al_2O_3 hybrid phase. The diffraction peaks of NiO and $NiCr_2O_4$ can also be observed in XRD pattern because the integrity of the oxide scale is destroyed after oxidation for 100 h, which leads to the exposure and oxidation of the middle layer of coating.

According to the analyses, it is found that the structure of the oxide scale formed on the DZ125 alloy is loose and porous without any protection to the substrate. The Cr-Al coatings with and without Y addition show better oxidation resistance than the bare DZ125 alloy does during oxidation at 1100 °C. Particularly, the Cr-Al-Y coating forms a dense oxide scale

Table 1 Chemical composition of the marked points in Fig.5a (at%)

Point	Al	Cr	Co	Ni	Y	Ta	W	Hf	Mo	Ti
1	19.3	13.0	5.8	58.8	-	0.9	1.8	-	-	0.4
2	16.9	15.7	6.1	55.1	0.3	1.8	3.4	-	-	0.7
3	17.3	10.3	7.0	56.7	0.1	2.7	4.9	0.2	0.1	0.7

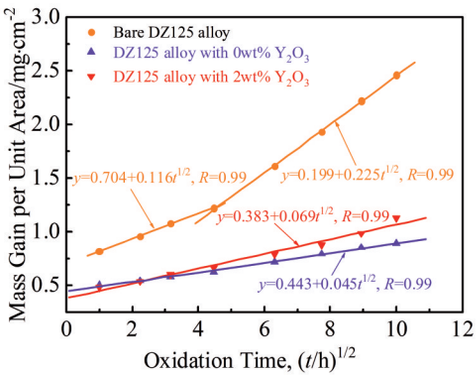

Fig.6 Oxidation kinetics of bare DZ125 alloy and DZ125 alloy with coating of 0wt% and 2wt% Y_2O_3 at 1100 °C in air

after oxidation, which consists of Cr_2O_3 and Al_2O_3 and is fully adherent to the coating.

Generally, there is close correlation between the formation/growth of oxide scale and the standard Gibbs free energy of formation (ΔG_f^θ) of oxides: the lower the ΔG_f^θ of oxide scale, the stronger the oxygen affinity[23]. ΔG_f^θ of different oxide scales with 1 mol O_2 at 1100 °C is arranged from the smallest to the largest: ΔG_f^θ (Y_2O_3) = − 1006.2 kJ/mol, ΔG_f^θ(Al_2O_3) = −825.5 kJ/mol, ΔG_f^θ (Cr_2O_3)=−518.7 kJ/mol, and ΔG_f^θ(NiO)= −232.8 kJ/mol.

Since ΔG_f^θ (Cr_2O_3) is low and the Cr content of the outer layer exceeds 85at%, Cr in the Cr+Ni_3Cr_2 outer layer forms a single Cr_2O_3 scale in the initial stage. Meanwhile, the Al atoms in the middle layer diffuse outwards under the concentration

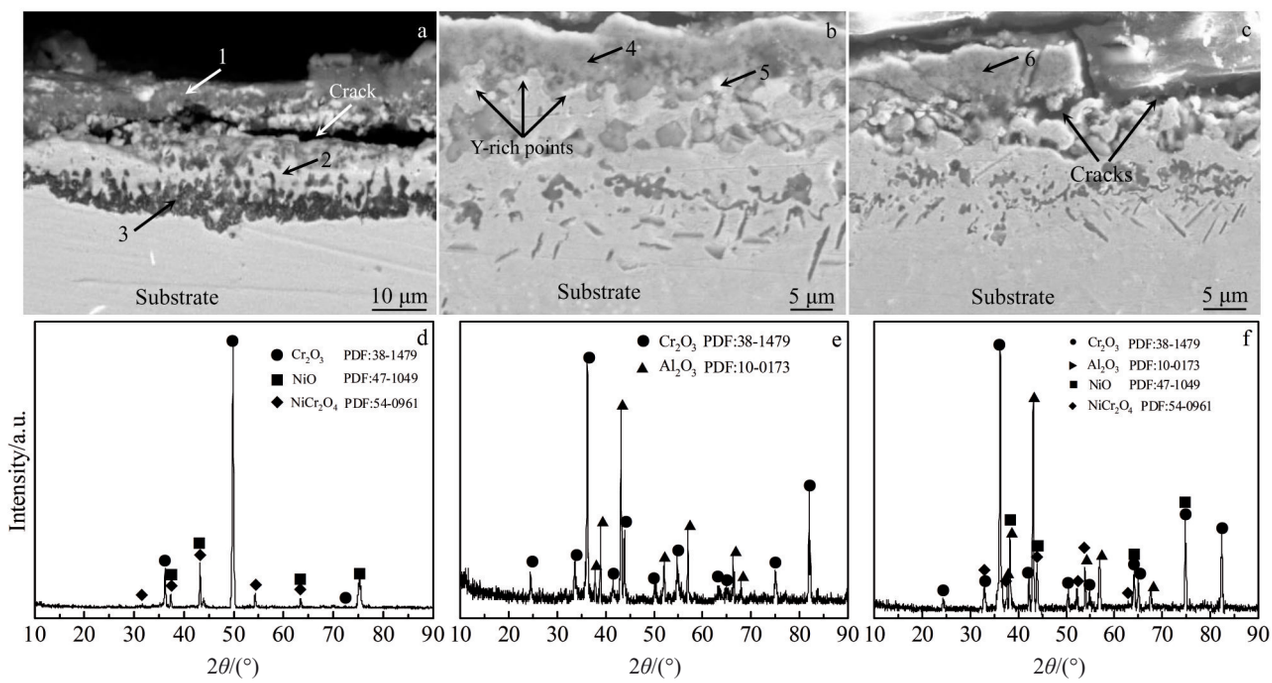

Fig.7 SEM-BSE cross-section morphologies (a−c) and XRD patterns (d−f) of DZ125 alloys with/without coatings after oxidation at 1100 °C: (a, d) bare DZ125 alloy after oxidation for 30 h; (b, e) DZ125 alloy with 2wt% Y_2O_3 coating after oxidation for 100 h; (c, f) DZ125 alloy with 0wt% Y_2O_3 coating after oxidation for 100 h

gradient, and then form the Al_2O_3 scale. As shown in Fig. 7b, some Y-rich particles form at the scale/coating interface, which generates a “keying” or “pegging” effect, therefore restraining the outward diffusion of cations (Ni atoms) from coatings[24]. Thus, the thermal stresses induced by the mismatch of thermal expansion coefficients between the coating and oxide scale during oxidation are reduced, and the adhesion of the oxide scale is enhanced significantly[25–26].

In conclusion, the Cr_2O_3 and Al_2O_3 scale can effectively prevent the entry of O atoms and thereby enhance the oxidation resistance of the substrate at high temperatures to a large extent, suggesting the positive effects of the Y addition in the coatings.

3 Conclusions

1) Cr-Al coatings on DZ125 alloy consist of a three-layered structure, regardless of with or without the Y addition: a Cr+Ni_3Cr_2 outer layer, a Ni_3Cr_2+$Al_{13}Co_4$ middle layer, and a Ni_3Al inner layer.

2) The Y_2O_3 content greatly influences the coating thickness and density. The coating thickness and density are increased obviously after the addition of Y_2O_3 in the pack mixtures. However, the excess addition of Y_2O_3 (5wt%) results in decreased coating thickness and density.

3) Cr-Al-Y co-deposition treatment significantly enhances the oxidation resistance of DZ125 alloy, which is attributed to the formation of a dense oxide scale consisting of Cr_2O_3 and

Al_2O_3. The oxide scale on the costing surface protects the DZ125 alloy during oxidation at 1100 °C for at least 100 h in air. The high-temperature oxidation resistance of DZ125 alloy is significantly improved by the coating with 2wt% Y_2O_3 addition. The oxidation resistance of DZ125 alloy with coating without Y_2O_3 addition is better than that of the bare DZ125 alloy, but it is worse than that with 2wt% Y_2O_3 addition.

References

1 Zang J J, Song P, Feng J *et al*. *Corrosion Science*[J], 2016, 112: 170

2 Pei Y W, Zhou C G. *Corrosion Science*[J], 2016, 112: 710

3 Hu X A, Yang X G, Shi D Q *et al. Chinese Journal of Aeronautics*[J], 2016, 29(1): 257

4 Li X, Guo X P, Qiao Y Q. *Transactions of Nonferrous Metals Society of China*[J], 2016, 26(7): 1892

5 Lin N M, Zhao L L, Liu Q *et al*. *Journal of Physics and Chemistry of Solids*[J], 2019, 129: 387

6 Yang X G, Li S L, Qi H Y. *International Journal of Fatigue*[J], 2015, 75: 126

7 Li S L, Yang X G, Qi H Y *et al*. *Materials Science and Engineering A*[J], 2016, 678: 57

8 Sun J B, Wang J S, Dong S J *et al*. *Journal of Alloys and Compounds*[J], 2018, 739: 856

9 Lin N M, Guo J W, Xie F Q *et al*. *Applied Surface Science*[J], 2014, 311: 330

10 Luo S H, He W F, Zhou L C *et al*. *Surface and Coatings Technology*[J], 2018, 342: 29

11 Hu G X, Xu Z X, Liu J J *et al*. *Surface and Coatings Technology*[J], 2009, 203: 3392

12 Liu R D, Jiang S M, Yu H J *et al*. *Corrosion Science*[J], 2016, 104: 162

13 Zhao X S, Zhou C G. *Corrosion Science*[J], 2014, 86: 223

14 Qi Yanfei, Ren Xiqiang, Zhou Jingyi *et al*. *Rare Metal Materials and Engineering*[J], 2022, 51(2): 735 (in Chinese)

15 Li Y Q, Xie F Q, Li X. *Journal of Wuhan University of Technology*: *Materials Science*[J], 2018, 33(4): 959

16 Tian X D, Guo X P. *Surface and Coatings Technology*[J], 2009, 204(1–2): 313

17 Li Y Q, Xie F Q, Wu X Q *et al*. *Applied Surface Science*[J], 2013, 287: 30

18 Li Y Q, Xie F Q, Wu X Q. *Transactions of Nonferrous Metals Society of China*[J], 2015, 25(3): 803

19 Lin N M, Xie F Q, Zhong T *et al*. *Journal of Rare Earths*[J], 2010, 28(2): 301

20 Lin N M, Xie F Q, Wu X Q. *Journal of Rare Earths*[J], 2011, 29(4): 396

21 Qiao Y Q, Guo X P. *Applied Surface Science*[J], 2010, 256(24): 7462

22 Zhang J Z, Yang Z L, Wei K Y. *Materials Review*[J], 2006, 20(5): 223

23 Lambert N, Borowiec K. *Journal of Alloys and Compounds*[J], 2000, 297(1–2): 266

24 Xiang J Y, Xie F Q, Wu X Q *et al*. *Vacuum*[J], 2020, 174: 109 190

25 Li X, Guo X P, Qiao Y Q. *Oxidation of Metals*[J], 2015, 83(3–4): 253

26 Zhang P, Guo X P. *Corrosion Science*[J], 2011, 53(1): 429

Y_2O_3对DZ125合金表面Cr-Al-Y渗层的组织结构及抗氧化性能影响

李涌泉[1,2]，田兴达[2]，王存喜[2]，李　轩[3]，杨少林[2]

(1. 北方民族大学 机电工程学院，宁夏 银川 750021)

(2. 北方民族大学 材料科学与工程学院，宁夏 银川 750021)

(3. 四川轻化工大学 机械工程学院，四川 自贡 643000)

摘　要：为进一步提高DZ125合金高温服役性能，通过扩散渗方法在其表面制备了稀土元素Y改性的Cr-Al共渗层，研究了Y_2O_3含量对渗层组织结构及抗高温氧化性能的影响。结果表明：不同条件下制备的Cr-Al-Y渗层均具有三层结构，由外向内依次为：Cr+Ni_3Cr_2外层，Ni_3Cr_2+$Al_{13}Co_4$中间层，以及Ni_3Al内层。当渗剂中Y_2O_3含量为0%~2%（质量分数，下同）时，渗层的厚度与密度显著增加；当稀土Y_2O_3的添加量过高时（5%），渗层的密度及厚度反而下降。1100 ℃高温氧化实验表明，Cr-Al-Y渗层显著提高了DZ125合金的抗高温氧化性能。

关键词：DZ125合金；Cr-Al-Y共渗层；Y_2O_3；抗高温氧化

作者简介：李涌泉，男，1985年生，博士，副教授，北方民族大学机电工程学院，宁夏 银川 750021，E-mail：2014141@nmu.edu.cn